This is the accepted manuscript made available via CHORUS. The article has been published as:

Effect of curvature and confinement on the Casimir-Polder interaction

Pablo Rodriguez-Lopez, Thorsten Emig, Ehsan Noruzifar, and Roya Zandi

Phys. Rev. A **91**, 012516 — Published 30 January 2015

DOI: 10.1103/PhysRevA.91.012516

Effect of Curvature and Confinement on the Casimir-Polder Interaction

Pablo Rodriguez-Lopez and Thorsten Emig
Laboratoire de Physique Théorique et Modèles Statistiques, CNRS UMR 8626, Bât. 100, Université Paris-Sud, 91405 Orsay cedex, France

Ehsan Noruzifar
Department of Chemistry and Biochemistry and Department of Physics, University of California, Santa Barbara, California 93106-9510, USA.

Roya Zandi
Department of Physics and Astronomy, University of California, Riverside, California 92521, USA

Modifications of Casimir-Polder interactions due to confinement inside a cylindrical cavity and due to curvature in- and outside the cavity are studied. We consider a perfectly conducting cylindrical shell with a single particle (atom or macroscopic sphere) located next to its interior or exterior surface, or two atoms placed inside the shell. By employing the scattering approach, we obtain the particle-cavity interaction and the modification of the two-particle interaction due to the cavity. We consider both retardation and thermal effects. While for the atoms a dipole description is sufficient, for the macroscopic sphere we sum (numerically) over many multipole fluctuations to compute the interaction at short separations. In the latter limit we compare to the proximity approximation and a gradient expansion and find agreement. Our results indicate an confinement induced suppression of the force between atoms. General criteria for suppression and enhancement of Casimir interactions due to confinement are discussed.

PACS numbers: 45.70.-n, 45.70.Mg

I. INTRODUCTION

Fluctuation-induced interactions between polarizable particles such as the London force [1] and its retarded companion, the Casimir-Polder force [2], play an ubiquitous role in fundamental physics, chemistry and applied technologies including nanotechnology and ultra-cold atomic systems [3–5]. A quantitative understanding of such forces is a key parameter in the design of new experiments and technological applications.

An important line of research addresses the dependence of these interactions on geometry and shape of the polarizable objects. Examples include the effect of surface curvature [6], sharp edges and tips [7], orientation dependence [8], and confinement [9, 10]. The non-additivity of fluctuation induced forces complicates the study of these effects. To overcome this problem, a multiscattering formalism for Casimir forces has been developed [11–15] and applied successfully [16–21], including the case of a sphere outside a cylinder [22, 23].

In this paper we use the scattering approach to investigate the Casimir forces between particles (atoms or a metallic sphere) placed inside a cylindrical cavity. In particular, our goal is to study how curvature and confinement modify the fluctuation-induced interactions between an atom and a curved surface and between atoms confined in perfectly conducing cylindrical cavities. Our results apply to both the zero temperature and the classical high temperature limit.

We find that in all cases, the interaction is considerably decreased compared to that in free space and decays exponentially over the scale of radius of the cylinder. This is mainly due to the fact that the fluctuation-induced forces are not pairwise additive. We obtain both a large and a short distance expansion for the force between an atom that is placed either inside or outside a cylindrical cavity.

Mahanty and Ninham studied the interaction between two atoms but confined between two parallel perfect metal plates [24] and found that at zero temperature the interaction energy was reduced from the free space case with an exponential decay in the non-retarded limit, and increased in the retarded case with a change from h^{-7} to $L^{-2}h^{-5}$ when h is much bigger than the distance L between the plates. For the same geometry, an exponential decay was also found at any finite temperature [25]. An exponential reduction of the interaction between the atoms has been also observed when they are confined in a rectangular waveguide and their distance is large compared to the diameter of the waveguide [26]. Contrary to that, a recent study of two atoms placed inside a transmission line consisting of two concentric metallic cylinders demonstrated a huge amplification of the interaction between the atoms due to the one-dimensional character of propagating fluctuations in this geometry [27].

All these studies confirm the importance of understanding the mechanism that determines the effect of confinement on the fluctuation-induced interactions. It seems that a massive fluctuation mode leads to an exponential decay of the associated interaction energy. In waveguides, massive modes are realized by evanescent modes due to the existence of finite cutoff frequencies for these modes. The study performed in this paper shows an exponential reduction of the interaction confirming that all modes in our cylindrical shell similar to those in the rectangular waveguide of Ref. [26] are massive. However, for two parallel conducting plates, there exists a massless mode only for TM polarization [28]. Since this propagating mode contributes for two particles with electric polarizability only in the retarded limit, the interaction is not exponentially suppressed but enhanced in this limit. Hence the situation resembles that of the transmission line.

We find that the interaction of atoms (or objects described by their electric and/or magnetic dipolar polarizabilities) close to cylindrical surfaces can be written as a small curvature expansion around the plate-atom case, in addition, the close similarity of the interior and exterior results suggest that they can be described by an analytical formula in the curvature of the surface. Going beyond the small particle limit, we consider the interaction of a macroscopic perfect metal sphere with the wall of a confining cylindrical shell. We find that the force on an object at short distances from the confining walls is modified by curvature and the force between two particles at large distances (compared to the confinement scale) is different from the force in free space. The comparison of our numerical results with a gradient expansion of the interaction demonstrates nice agreement at small separations. For the interaction between two atoms that are placed on the axis of a confining cylindrical shell we derive exact results in the asymptotic limit of large separations both at zero and high temperatures.

Understanding the modifications in the Casimir force resulting from confinement could explain the rate of chemical reactions contained in carbon nanotubes [29], and could shed the light on processes leading to an increase or a reduction of the Casimir force in these systems.

The remainder of the article is organized as follows: In Sec. II we briefly review the multiscattering approach used to obtain Casimir interactions. In Sec. III we analyze the retarded and non-retarded Casimir interaction between an atom and a perfect metal cylindrical cavity, both in the high and low temperature limits. Interior and exterior cases are considered. In Sec. IV A the proximity force approximation (PFA) for a perfect metal sphere inside a perfect metal cylindrical cavity is given. In Sec. IV B, the Casimir interaction for the latter geometry is computed numerically and compared to the PFA and a gradient expansion. In Sec. V, the confinement of two atoms is studied by computing their interaction along the axis of a perfect metal cylindrical cavity. We conclude with a discussion of our results, and a summary of relevant matrix elements is given in App. A.

II. SCATTERING APPROACH

We employ the scattering approach [11, 12] to compute the Casimir interactions. This approach relates the interaction between objects to their electromagnetic scattering properties. The Casimir free energy at temperature T is given by

$$E = k_B T \sum_{n=0}^{\infty}{}' \log\det[\mathcal{I} - \mathcal{N}(\kappa_n)], \tag{1}$$

where $\kappa_n = 2\pi n k_B T/\hbar c$ are Matsubara wave numbers. The prime indicates that the zero Matsubara frequency contribution has a weight of $1/2$. At zero temperature, the primed sum is replaced by an integral along the imaginary frequency axis, yielding the Casimir energy

$$E_0 = \frac{\hbar c}{2\pi} \int_0^{\infty} d\kappa \log\det[\mathcal{I} - \mathcal{N}(\kappa)]. \tag{2}$$

The high temperature or classical limit is reached when the distance between the interacting objects becomes much larger than the thermal wavelength $\lambda_T = \hbar c/(k_B T)$. The Casimir free energy is then given by the zero Matsubara frequency term of Eq. (1),

$$E_{cl} = \frac{k_B T}{2} \log\det[\mathcal{I} - \mathcal{N}(0)]\,. \tag{3}$$

Following the notation of [9, 12], the blocks forming the matrix $\mathcal{N}$ for a geometry consisting of a finite number of objects are given by

$$(\mathcal{I} - \mathcal{N})_{\alpha\beta} = \delta_{\alpha\beta} + (1 - \delta_{\alpha\beta})\mathcal{T}_\alpha \mathcal{X}_{\alpha\beta}, \tag{4}$$

where α and β label the interacting bodies. $\mathcal{T}_\alpha$ is the T-matrix of object α (either the cavity or an object inside), and it encodes all information about shape and material composition of the object. We are interested in a situation where objects are entirely enclosed within the cavity formed by an external object which will be a cylindrical shell. The T-matrix of the external object relevant to this situation of internal scattering is different from the T-matrix of the same object for external scattering. The latter case is relevant to objects placed outside the cylinder. For perfectly conducting boundary conditions, the T-matrix for internal scattering is the inverse of the T-matrix for external scattering. The translation matrices $\mathcal{X}_{\alpha\beta}$ describe the interaction of the fluctuating multipole moments on object α and β. They contain all information about the relative position and orientation of the objects. If $\mathcal{X}_{\alpha\beta}$ connects two separate objects (both either inside or outside of a cavity), we have $\mathcal{X}_{\alpha\beta} = \mathcal{U}_{\alpha\beta}$, where the matrix $\mathcal{U}_{\alpha\beta}$ relates regular waves to outgoing waves [12]. When $\mathcal{X}_{\alpha\gamma}$ connects a body α to the external cavity $\gamma = C$ (C will denote the cavity in the following) enclosing it, we have $\mathcal{X}_{\alpha C} = \mathcal{V}_{\alpha C}$ where the matrix $\mathcal{V}_{\alpha C}$ connects regular waves (with respect to the origin of coordinates) of the object α to regular waves of the cavity C [12]. Finally, if $\mathcal{X}_{C\beta}$ connects the enclosing cavity C with a body β placed in its interior, we have $\mathcal{X}_{C\beta} = \mathcal{W}_{C\beta}$, relating now regular waves of the cavity C to regular waves of β, with $\mathcal{W}^{ij}_{C\beta} = \mathcal{V}^{\dagger\, ij}_{\beta C} \frac{C_i}{C_j}$ where the generalized indices i, j label the multipole waves including polarization, and C_i are normalization constants [12]. For the configuration of one object S inside or outside the cavity C, the matrix $\mathcal{N}$ is given by

$$\mathcal{N} = \mathcal{T}_S \mathcal{X}_{SC} \mathcal{T}_C \mathcal{X}_{CS}\,. \tag{5}$$

The T-matrix of object S and the cavity C are usually given in different vector multipole basis. Therefore, we have to apply a change of basis to one of the T-matrices in order to apply the above formula. Since here the cavity is a cylindrical shell and the particle S has spherical symmetry (atom or sphere), we shall use the conversion matrices $D_{l,m,P,n,k_z,Q}$ of spherical vector waves $\phi_{l,m,P}$ into cylindrical vector waves $\phi_{n,k_z,Q}$ defined by [22]

$$\phi_{l,m,P} = \sum_{n\in\mathbb{Z}} \sum_{Q=M,N} \int_{-\infty}^{\infty} \frac{dk_z}{2\pi} D_{l,m,P,n,k_z,Q}\, \phi_{n,k_z,Q}\ , \tag{6}$$

where Q denotes electric (N) or magnetic (M) polarizations. By the use of these conversion matrices, the T-matrix of object

S (given in spherical wave basis) can be transformed to the cylindrical vector basis as [12]

$$\mathcal{T}_{S\ n\,k_z\,P,n'\,k'_z\,P'} = \sum_{l,m,Q}\sum_{l',m',Q'} \frac{C^c_P}{C^s_Q} D^\dagger_{n\,k_z\,P,lmQ} \times \mathcal{T}_{S\ l\,m\,Q,l'\,m'\,Q'} D_{l'\,m'\,Q',n'\,k'_z\,P'}, \quad (7)$$

where we have used $C^c_M = -\frac{1}{2\pi} = -C^c_N$ and $C^s_M = \kappa = -C^s_N$ to obtain $C^c_P/C^s_Q = (2\pi\kappa)^{-1}(1-2\delta_{P,Q})$ [12] (see also App. A). Now the matrix $\mathcal{N}$ for a compact object inside a cylindrical cavity can be expressed in spherical vector wave basis as

$$\mathcal{N}_{l'm',lm} = \frac{1}{4\pi^2\kappa}\mathcal{T}_{S\ l'm',lm}\int_{-\infty}^{\infty} dk_z D_{lm,nk_z} \times \mathcal{V}_{SC\ nk_z,n'k'_z}\mathcal{T}_{C\ n'k'_z,n''k''_z}\mathcal{V}^\dagger_{CS\ n''k''_z,\tilde{n}\tilde{k}_z} D^\dagger_{\tilde{n}\tilde{k}_z,lm}, \quad (8)$$

with summation over repeated indices. Note that the polarization indices are not explicitly shown. Details about the matrices used in Eq. (8) can be found in App. A. The energies defined by Eqs. (1), (2) and (3) are finite for all positions of the internal object inside the cylinder. Therefore, a regularization is not needed, in contrast to the interaction of two exterior objects where the energy for infinite distance is usually subtracted.

III. CASIMIR ENERGY OF AN ATOM AND A METALLIC CYLINDER

In this section we calculate the Casimir energy of an atom that is placed outside or inside an infinitely long perfect metal cylindrical cavity. We obtain analytical results in asymptotic regimes, and numerical results for intermediate distances. Our results are based on two assumptions: (1) The atom is described by its electric and magnetic dipolar polarizabilities α_E and α_M, respectively, and has no higher multipole polarizabilities, and (2) the polarizabilities are small compared to all geometric length scales, i.e., $\alpha_P^{1/3} \ll d, R_c, \ell$, being d, R_c and ℓ the distance from the atom to the center of the cylinder, the radius of the cylinder and the distance from the atom to the cylindrical surface respectively (the lenght of the cylinder L is always assumed to be much larger than the rest of lengths of the system). These assumptions are frequently made in the literature, leading to the Casimir-Polder interaction between a flat surface and an atom [2]. The second assumptions justifies to consider only one scattering at the atom so that the energy is linear in α_P, and hence we keep only the linear term in

$$\log\det\left[\mathcal{I}-\mathcal{N}\right] = -\mathrm{Tr}\left[\mathcal{N}\right] + \mathcal{O}(\mathcal{N}^2)\,. \quad (9)$$

The first assumption implies that the trace runs only over dipolar waves ($l=1$), yielding

$$\mathrm{Tr}\left[\mathcal{N}\right] = \frac{1}{4\pi^2\kappa}\mathcal{T}_{S\,1,m,P;1,m',P'} D_{1,m',P';n,k_z,P''} \times \mathcal{X}_{SC,\ n,k_z,P'';n',k'_z,Q}\mathcal{T}_{C\ n',k'_z,Q;n'',k''_z,Q'} \times \mathcal{X}_{CS,\ n'',k''_z,Q';\tilde{n},\tilde{k}_z,Q''} D^\dagger_{\tilde{n},\tilde{k}_z,Q'';1,m,P}, \quad (10)$$

where summation over all discrete indices and integration over all wave vectors along the z-axis is assumed. Here $\mathcal{T}_S$ represents the atom (for the T-matrix of an atom, see App. A.) In the following we shall apply these general results to a perfectly conducting cylindrical cavity.

A. Retarded Casimir-Polder energy of an atom inside a cylinder

1. *Zero temperature limit*

The Casimir energy at zero temperature of the atom placed at a distance $d < R_c$ from the axis of the cylindrical shell of radius R_c can be written as

$$E_0 = -\frac{\hbar c}{R_c^4}\left(f_0^E(\delta)\alpha_E + f_0^M(\delta)\alpha_M\right), \quad (11)$$

where $\delta = d/R_c$. The dependence on δ is determined by the following auxiliary functions

$$\mathcal{I}^P_{\alpha,m}(\delta) = \int_0^\infty dt\, t^\alpha \sum_{n\in\mathbb{Z}} I^2_{n+m}(t\delta)\mathcal{T}_{C\ n,P;n,P}(t), \quad (12)$$

with the Bessel function I_n and where $\mathcal{T}_C$ is the T-matrix that describes the scattering inside the perfectly conducting cylindrical shell where the integration variable t stands for the rescaled expression $\sqrt{\kappa^2+k_z^2}$. The diagonal matrix elements are given by (see App. A)

$$\mathcal{T}_{C\ n,M;n,M}(t) = -\frac{K'_n(t)}{I'_n(t)}\,, \quad (13)$$

$$\mathcal{T}_{C\ n,N;n,N}(t) = -\frac{K_n(t)}{I_n(t)}\,. \quad (14)$$

The amplitudes $f_0^E(\delta)$ and $f_0^M(\delta)$ are then given by

$$f_0^E(\delta) = \frac{1}{4\pi}\left(\mathcal{I}^M_{3,1}(\delta) - \mathcal{I}^N_{3,1}(\delta) - 2\mathcal{I}^N_{3,0}(\delta)\right)\,, \quad (15)$$

$$f_0^M(\delta) = -\frac{1}{4\pi}\left(\mathcal{I}^M_{3,1}(\delta) - \mathcal{I}^N_{3,1}(\delta) + 2\mathcal{I}^M_{3,0}(\delta)\right)\,. \quad (16)$$

Using the uniform asymptotic expansion for Bessel functions as employed in [30], we obtain for *small* atom-surface distance $\ell = R_c - d$ the expansion

$$f_0^E = \frac{3}{8\pi}\left(\frac{R_c}{\ell}\right)^4 + \frac{13}{60\pi}\left(\frac{R_c}{\ell}\right)^3 + \frac{311}{1680\pi}\left(\frac{R_c}{\ell}\right)^2 + \cdots\,, \quad (17)$$

$$f_0^M = -\frac{3}{8\pi}\left(\frac{R_c}{\ell}\right)^4 - \frac{17}{60\pi}\left(\frac{R_c}{\ell}\right)^3 - \frac{431}{1680\pi}\left(\frac{R_c}{\ell}\right)^2 + \cdots\,. \quad (18)$$

The leading term agrees with the Casimir-Polder interaction between an atom and a planar surface [2]. The sub-leading terms describe curvature corrections. The first correction term for the E polarization has been obtained in Ref. [30].

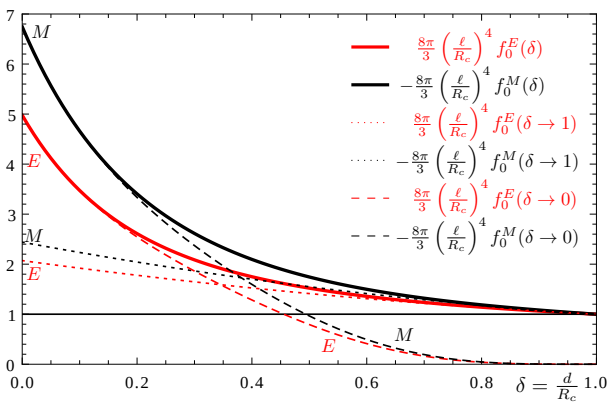

Figure 1. (Color online). Amplitudes of the interior Casimir-Polder interaction between an atom and a cylindrical shell as function of $\delta = d/R_c$. Shown are the limiting analytical results for short distances (dotted curves, see Eqs. (17), (18)), and when the atom is close to the axis of the cylinder (dashed curves, see Eqs. (19), (20)). The thick curves correspond to the full numerical result for $f_0^E(\delta)$ (Eq. (15)) and $f_0^M(\delta)$ (Eq. (16)).

When the atom is close to the center of the cylinder ($\delta \ll 1$), one can expand the functions $\mathcal{I}^P_{\alpha,m}(\delta)$ for small δ and perform the integral over t and infinite sum over n numerically. The result is

$$f_0^E(\delta) = \quad 0.594032 + 3.67884\,\delta^2 + \mathcal{O}(\delta^4)\,, \tag{19}$$

$$f_0^M(\delta) = -0.805032 - 4.15129\,\delta^2 + \mathcal{O}(\delta^4)\,. \tag{20}$$

Note that for atoms without magnetic response ($\alpha_M = 0$ and $\alpha_E > 0$), the Casimir-Polder interaction is attractive, while for (fictive) atoms without electric response ($\alpha_E = 0$ and $\alpha_M > 0$), the interaction is repulsive. This is in agreement with the interaction between an atom and a flat surface. Hence, surface curvature does not change the sign of the interaction.

The analytical results for the atom placed either close to the cylindrical surface or close to its axis are shown in Fig. 1 together with numerical results valid for all distances δ. This comparison shows that the two limiting results provide an accurate estimate of the interaction over a wide range of separations.

2. *High temperature limit*

When $d \gg \lambda_T$, the Casimir energy can be approximated by its high temperature limit, given by Eq. (3). For an atom inside a cylindrical cavity, this expressions reduces to

$$E_{cl} = -\frac{k_B T}{2}\mathrm{Tr}\left[\mathcal{N}(0)\right]\,, \tag{21}$$

which can be written as

$$E_{cl} = -\frac{k_B T}{R_c^3}\left(f_{cl}^E(\delta)\alpha_E + f_{cl}^M(\delta)\alpha_M\right)\,, \tag{22}$$

The amplitudes $f_{cl}^E(\delta)$ and $f_{cl}^M(\delta)$ can be expressed in terms of $\mathcal{I}^P_{\alpha,m}(\delta)$ defined in Eq. (12) as

$$f_{cl}^E(\delta) = -\frac{1}{\pi}\left(\mathcal{I}^N_{2,1}(\delta) + \mathcal{I}^N_{2,0}(\delta)\right)\,, \tag{23}$$

$$f_{cl}^M(\delta) = -\frac{1}{\pi}\left(\mathcal{I}^M_{2,1}(\delta) + \mathcal{I}^M_{2,0}(\delta)\right)\,. \tag{24}$$

Using again the uniform asymptotic expansion for Bessel functions, we obtain the asymptotic behavior of $\mathcal{I}^P_{\alpha,m}(\delta)$ when the atom is close to the surface of the cavity. This yields the amplitudes for $\ell \ll R_c$,

$$f_{cl}^E = \frac{1}{4}\left(\frac{R_c}{\ell}\right)^3 + \frac{1}{8}\left(\frac{R_c}{\ell}\right)^2 + \frac{1}{8}\left(\frac{R_c}{\ell}\right) + \cdots\,, \tag{25}$$

$$f_{cl}^M = -\frac{1}{4}\left(\frac{R_c}{\ell}\right)^3 - \frac{1}{4}\left(\frac{R_c}{\ell}\right)^2 - \frac{1}{4}\left(\frac{R_c}{\ell}\right) + \cdots\,. \tag{26}$$

The leading terms describe the atom-planar surface interaction, and the additional terms are curvature corrections.

When the atom is close to the axis of the cylindrical cavity, a small δ expansion and subsequent numerical summation and integration yields the amplitudes

$$f_{cl}^E(\delta) = \quad 1.00274 + 4.00376\,\delta^2 + \mathcal{O}(\delta^4)\,, \tag{27}$$

$$f_{cl}^M(\delta) = -1.79579 - 5.06599\,\delta^2 + \mathcal{O}(\delta^4)\,. \tag{28}$$

We have also evaluated numerically the amplitudes of Eqs. (23) and (24). The results, and the approximations for small ℓ and small δ are shown in Fig. 2.

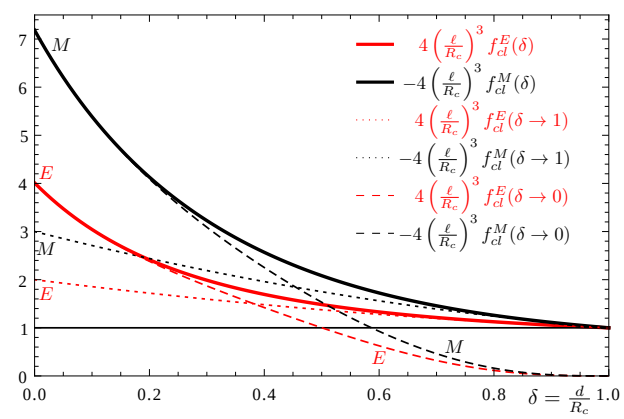

Figure 2. (Color online). Equivalent of Fig. 1 for the classical limit. Shown are the analytical results for short surface distances ℓ (dotted curves, see Eqs. (25), (26)), and when the atom is close to the axis of the cylinder (dashed curves, see Eqs. (27), (28)). The thick curves represent the full numerical result for $f_{cl}^E(\delta)$ (Eq. (23)) and $f_{cl}^M(\delta)$ (Eq. (24)).

B. Non-retarded London energy of an atom inside the cylinder

So far we have considered the retarded limit where the distance $d \gg d_{10}$ is much bigger than the retardation length

$d_{10} = c/\omega_{10}$ set by the transition frequency of a two-state atom (see App. A for its polarizability). Next we shall assume the opposite limit where $d \ll d_{10}$ which can be realized to leading order by taking the limit $c \to \infty$. The resulting interaction is known as London force. In the following we consider finite temperatures so that to leading order in d/d_{10} one has

$$E_T^L = -\lim_{c\to\infty} k_B T {\sum_{n=0}^{\infty}}' \mathrm{Tr}\left[\mathcal{N}(\kappa_n)\right] . \tag{29}$$

Here for need to substitute for the polarizability of the atom the frequency dependent expression of Eq. (A10). Then the matrix $\mathcal{N}(\kappa_n)$ depends on the combinations $d\kappa_n$, $R_c\kappa_n$ and $d_{10}\kappa_n = 2\pi n k_B T/(\hbar\omega_{10})$. The first two combinations scale as $1/c$ and hence tend to zero whereas the latter obviously remains finite for $c \to \infty$. Hence the non-retarded interaction is given by the Matsubara sum taken over two times the classical interaction energy E_{cl} of Eq. (22) with α_P replaced by $\alpha_P/[1+(2\pi n k_B T/(\hbar\omega_{10}))^2]$. The sum over n can be carried out easily, and one obtains the following result for the London interaction valid for all temperatures

$$E_T^L(\delta) = \frac{\hbar\omega_{10}}{2k_B T}\coth\left(\frac{\hbar\omega_{10}}{2k_B T}\right) E_{cl}(\delta). \tag{30}$$

This shows that the effect of geometry (curvature) in the non-retarded limit is fully determined by the geometry dependence in the classical limit. Note that, in the zero and high temperature limits of the London energy we have

$$E_0^L(\delta) = \frac{\hbar\omega_{10}}{2k_B T} E_{cl}(\delta), \quad E_{cl}^L(\delta) = E_{cl}(\delta). \tag{31}$$

C. Retarded Casimir-Polder energy of an atom outside a cylinder

1. *Zero temperature limit*

The Casimir potential at zero temperature of an atom outside a perfectly conducting cylinder at a distance d from the cylinder axis can be written as

$$E_0 = -\frac{\hbar c}{R_c^4}\left(g_0^E(\delta)\alpha_E + g_0^M(\delta)\alpha_M\right), \tag{32}$$

where $\delta = d/R_c$. The dependence on δ is determined by the integrals

$$\mathcal{K}^P_{\alpha,m}(\delta) = \int_0^\infty dt\, t^\alpha \sum_{n\in\mathbb{Z}} K^2_{n+m}(\delta t)\mathcal{T}_{C\,n,P;n,P}(t), \tag{33}$$

where $\mathcal{T}_C$ is the diagonal T–matrix that described the scattering outside the cylinder. The matrix elements are given by

$$\mathcal{T}_{C\,n,M;n,M}(t) = -\frac{I_n'(t)}{K_n'(t)}, \tag{34}$$

$$\mathcal{T}_{C\,n,N;n,N}(t) = -\frac{I_n(t)}{K_n(t)}. \tag{35}$$

Then the amplitudes $g_0^E(\delta)$ and $g_0^M(\delta)$ are given by

$$g_0^E(\delta) = \frac{1}{4\pi}\left(\mathcal{K}^M_{3,1}(\delta) - \mathcal{K}^N_{3,1}(\delta) - 2\mathcal{K}^N_{3,0}(\delta)\right), \tag{36}$$

$$g_0^M(\delta) = -\frac{1}{4\pi}\left(\mathcal{K}^M_{3,1}(\delta) - \mathcal{K}^N_{3,1}(\delta) + 2\mathcal{K}^M_{3,0}(\delta)\right). \tag{37}$$

Using again the uniform asymptotic expansion for Bessel functions, we find for *small* atom-surface distance $\tilde{\ell} = d - R_c$ the expansion

$$g_0^E = \frac{3}{8\pi}\left(\frac{R_c}{\tilde{\ell}}\right)^4 - \frac{13}{60\pi}\left(\frac{R_c}{\tilde{\ell}}\right)^3 + \frac{311}{1680\pi}\left(\frac{R_c}{\tilde{\ell}}\right)^2 + \cdots, \tag{38}$$

$$g_0^M = -\frac{3}{8\pi}\left(\frac{R_c}{\tilde{\ell}}\right)^4 + \frac{17}{60\pi}\left(\frac{R_c}{\tilde{\ell}}\right)^3 - \frac{431}{1680\pi}\left(\frac{R_c}{\tilde{\ell}}\right)^2 + \cdots. \tag{39}$$

which is consistent with [30]. Comparison with Eqs. (17), (18) shows that the interior and exterior cases are related by $R_c \to -R_c$. While an interior atom sees negative surface curvature, an exterior atom experiences positive curvature.

In the large distance limit, $d \gg R_c$, we obtain the following asymptotic amplitudes

$$g_0^E = \frac{1}{3\pi\ln(d/R_c)}\left(\frac{R_c}{d}\right)^4, \tag{40}$$

$$g_0^M = -\frac{1}{6\pi\ln(d/R_c)}\left(\frac{R_c}{d}\right)^4, \tag{41}$$

yielding for the Casimir potential

$$E_0 = -\frac{\hbar c(2\alpha_E - \alpha_M)}{6\pi\, d^4\ln(d/R_c)}. \tag{42}$$

Numerical and analytical results are compared in Fig. 3, where the convergence of the numerical data to the various limits is shown.

2. *High temperature limit*

We consider now high temperatures so that $d \gg \lambda_T$. Similar to the interior case, the Casimir potential can be written as

$$E_{cl}(r_c) = -\frac{k_B T}{R_c^3}\left(g_{cl}^E(\delta)\alpha_E + g_{cl}^M(\delta)\alpha_M\right). \tag{43}$$

The functions $g_{cl}^E(\delta)$ and $g_{cl}^M(\delta)$ can be written in terms of the functions $\mathcal{K}^P_{\alpha,m}(\delta)$ as

$$g_{cl}^E(\delta) = -\frac{1}{\pi}\left(\mathcal{K}^N_{2,1}(\delta) + \mathcal{K}^N_{2,0}(\delta)\right), \tag{44}$$

$$g_{cl}^M(\delta) = -\frac{1}{\pi}\left(\mathcal{K}^M_{2,1}(\delta) + \mathcal{K}^M_{2,0}(\delta)\right). \tag{45}$$

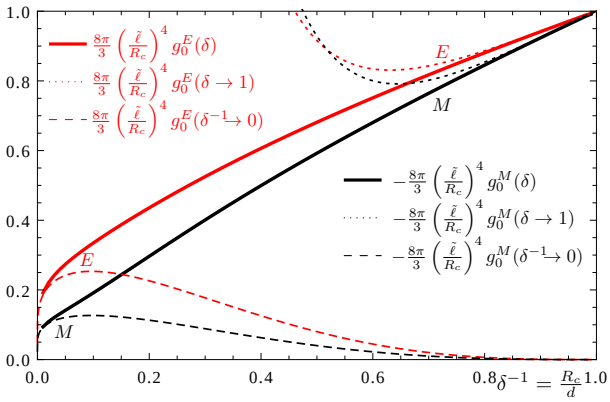

Figure 3. (Color online). Amplitudes of the exterior Casimir-Polder interaction between an atom and a cylindrical shell as function of $1/\delta = R_c/d$. Shown are the limiting analytical results for short distances (dotted curves, see Eqs. (38), (39)), and when the atom is far away from the cylinder (dashed curves, see Eqs. (40), (41)). The thick curves correspond to the full numerical result for $g_0^E(\delta)$ (Eq. (36)) and $g_0^M(\delta)$ (Eq. (37)).

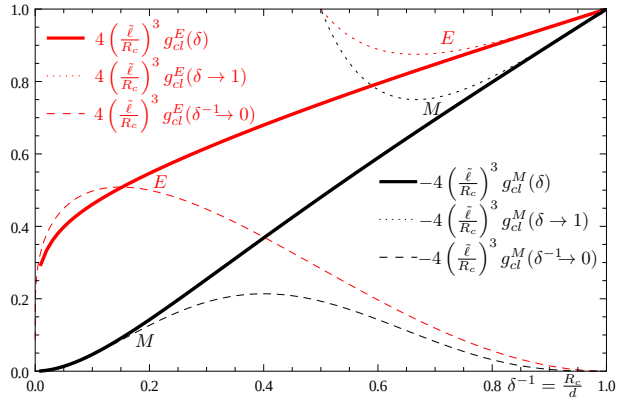

Figure 4. (Color online). Equivalent of Fig. 3 for the classical limit. Shown are the analytical results for short surface distances $\tilde{\ell}$ (dotted curves, see Eqs. (46), (47)), and when the atom is far away from the cylinder (dashed curves, see Eqs. (48), (49)). The thick curves represent the full numerical result for $g_{cl}^E(\delta)$ (Eq. (44)) and $g_{cl}^M(\delta)$ (Eq. (45)).

The asymptotic expansion of Bessel functions yields again the asymptotic behavior of $\mathcal{K}^P_{\alpha,m}$ when the atom is close to the surface of the cavity. In this limit we obtain

$$g_{cl}^E = \frac{1}{4}\left(\frac{R_c}{\tilde{\ell}}\right)^3 - \frac{1}{8}\left(\frac{R_c}{\tilde{\ell}}\right)^2 + \frac{1}{8}\left(\frac{R_c}{\tilde{\ell}}\right) + \cdots , \tag{46}$$

$$g_{cl}^M = -\frac{1}{4}\left(\frac{R_c}{\tilde{\ell}}\right)^3 + \frac{1}{4}\left(\frac{R_c}{\tilde{\ell}}\right)^2 - \frac{1}{4}\left(\frac{R_c}{\tilde{\ell}}\right) + \cdots . \tag{47}$$

This results is again related to the corresponding one for the interior case in Eqs. (25), (26) by $R_c \to -R_c$.

In the large distance limit, $d \gg R_c$, we find the asymptotic expressions

$$g_{cl}^E = \frac{\pi}{8\ln(d/R_c)}\left(\frac{R_c}{d}\right)^3 , \tag{48}$$

$$g_{cl}^M = -\frac{63\pi}{128}\left(\frac{R_c}{d}\right)^5 , \tag{49}$$

which yield the Casimir potential

$$E_{cl} = -\frac{k_B T \pi \alpha_E}{8 d^3 \ln(d/R_c)} . \tag{50}$$

Note that the leading asymptotic interaction is dominated by the electric response of the atom only. The results of all full numerical computation of the interaction at all distances is shown in Fig. 4 together with the analytically studied limits.

D. Non-retarded London energy of an atom outside the cylinder

In the non-retarded limit with $d \ll d_{10}$ for the exterior case of an atom outside the cylinder exactly the same relations as in the interior case hold, see Eqs. (30), (31).

IV. CASIMIR ENERGY OF A METAL SPHERE INSIDE A METAL CYLINDER

A. Proximity force approximation

In this section we come back to an interior situation. Instead of an atom, we place a macroscopic metallic sphere inside the cylinder. We assume that both the cylinder and the sphere are perfectly conducting, and have radii R_c and R_s, respectively. The sphere–center to cylinder–axis separation is $d \le R_c - R_s$. Before computing the exact interaction in the next section, we consider here the proximity force approximation (PFA). In general, the PFA energy $E_{\rm PFA}$ for two surfaces is given by

$$E_{\rm PFA} = \int dA\, E_{\parallel}(h) , \tag{51}$$

where $E_{\parallel}(h)$ is the energy per unit area for two parallel plates of distance h. In the above expression the integration is performed along one surface with h the local distance to the other surface. After integration, the result is expanded for small distances, and only the leading order is retained. To this order, the precise direction along which h is measured, is unimportant.

Assuming the origin at the axis of the cylinder (oriented along the x-axis), the position of a surface element on the cylinder is $(x_c, y_c = R_c\sin(\phi_c), z_c = R_c\cos(\phi_c))$, and the position of a surface element on the sphere is $(x_s = R_s\sin(\theta_s)\cos(\phi_s), y_s = R_s\sin(\theta_s)\sin(\phi_s), z_s = d + R_s\cos(\theta_s))$. The distance between the two surface elements then is

$$h = z_c - z_s . \tag{52}$$

The center-to-axis distance d is related to the minimal surface-to-surface distance ℓ between the sphere and the cylinder by

$d = R_c - (\ell + R_s)$. Hence Eq. (52) can be written as

$$h = \ell + R_s\,[1 - \cos(\theta_s)] - R_c\,[1 - \cos(\phi_c)]\,. \tag{53}$$

Next we express ϕ_c in terms of θ_s and ϕ_s, using $y_c = y_s$,

$$\sin(\phi_c) = \frac{R_s}{R_c}\sin(\theta_s)\sin(\phi_s)\,. \tag{54}$$

Using Eq. (54) in Eq. (53) and making use of the fact that at short separations, the surface elements of the sphere and cylinder for which $\theta_s \ll 1$ and $\phi_c \ll 1$ contribute most to the interaction, the local distance h can be approximated by

$$h(\theta_s, \phi_s) \approx \ell + \frac{R_s\theta_s^2}{2}\left[1 - \frac{R_s}{R_c}\sin^2(\phi_s)\right]\,. \tag{55}$$

We express Eq. (51) in terms of surface coordinates of the sphere,

$$E_{\rm PFA} = R_s^2 \int_0^{2\pi} d\phi_s \int_0^{\pi} d\theta_s \sin\theta_s\, E_{\parallel}(h)\,, \tag{56}$$

For small θ_s we use $\sin\theta_s \approx \theta_s$ and change the integration variable θ_s to H which is defined by the right hand side of Eq. (55) so that

$$\theta_s\, d\theta_s = \frac{dH}{R_s\left[1 - \frac{R_s}{R_c}\sin^2(\phi_s)\right]}\,. \tag{57}$$

This yields

$$E_{\rm PFA} = R_s\left[\int_0^{2\pi}\frac{d\phi_s}{1 - \frac{R_s}{R_c}\sin^2(\phi_s)}\right]\int_\ell^\infty dH\, E_{\parallel}(H)\,, \tag{58}$$

where we have moved the upper integration limit for H to infinity since this does not change the leading behavior of the integral for small ℓ. The integration over ϕ_s can be carried out easily and we obtain the PFA energy

$$E_{\rm PFA} = \frac{2\pi R_s}{\sqrt{1 - \frac{R_s}{R_c}}}\int_\ell^\infty dH\, E_{\parallel}(H)\,. \tag{59}$$

In particular, for perfect conductors, we obtain

$$E_{\rm PFA,0} = -\hbar c\frac{R_s}{\ell^2}\frac{\pi^3}{720\sqrt{1 - \frac{R_s}{R_c}}} \tag{60}$$

for zero temperature, and

$$E_{\rm PFA,cl} = -k_B T\frac{R_s}{\ell}\frac{\zeta(3)}{4\sqrt{1 - \frac{R_s}{R_c}}} \tag{61}$$

in the classical high temperature limit with $d \gg \lambda_T$.

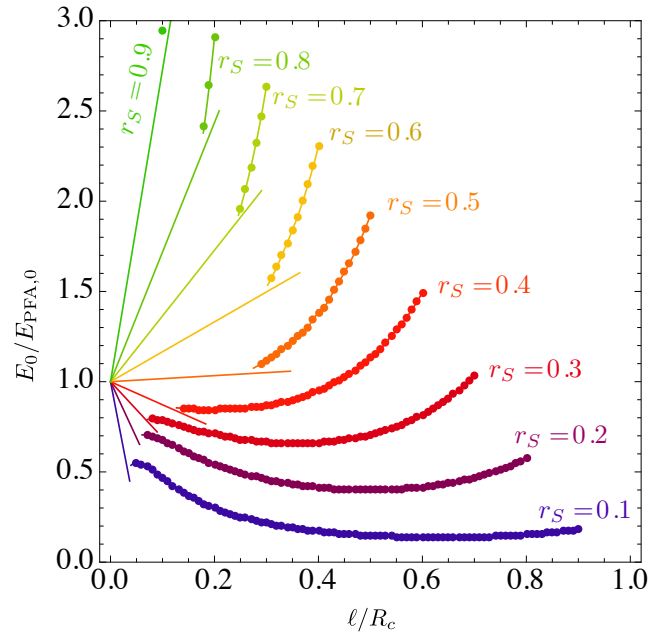

Figure 5. (Color online) Numerical result for the zero temperature Casimir energy (normalized to PFA) for a sphere inside a cylinder for different ratios of the radii, ranging from $r_s = R_s/R_c = 0.1$ (bottom blue) to $r_s = 0.9$ (top green) in steps of 0.1, as a function of $\ell/R_c < 1 - r_s$. The curves terminate at the positions where the sphere is located at the axis of the cylinder ($\ell/R_c = 1 - r_s$). The straight lines originating from unity represent the first correction to PFA, see Eq. (62).

B. Numerical result

Now we compute the interaction for the geometry of the previous section numerically at all distances, using the scattering approach. Again, we consider zero temperature and the classical high temperature limit. We obtain the Casimir energy numerically from the matrix $\mathcal{N}$ defined in Eq. (8) using Eqs. (2), (3). The T-matrix elements for a perfectly conducting cylinder and sphere are given in App. A. In order to perform the numerical calculations, we have restricted the vector spherical multipoles to $l \leq 20$ in the zero temperature case and to $l \leq 30$ in the high temperature case. The cylindrical multipoles are limited to $|n| \leq 500$. The results are shown in Fig. 5 ($T = 0$) and Fig. 6 (classical limit) as function of $\ell/R_c < 1 - R_s/R_c$ for different radii of the sphere. The data for the numerically computed Casimir energy are normalized to the PFA [see Eqs. (60), (61)].

The multipole expansion for Casimir interactions works best at large separations, and an increasing number of multipoles is required when the surfaces of the bodies approach each other. This is clearly visible in the numerical data that should converge to unity for $\ell \to 0$ when normalized to the PFA but fail to do so below $\ell/R_c \lesssim 0.05$. However, for $\ell/R_c \gtrsim 0.05$ we expect our numerical results to be reliable, and they clearly show strong deviations from the PFA when the sphere is moved towards the axis of the cylinder (reached

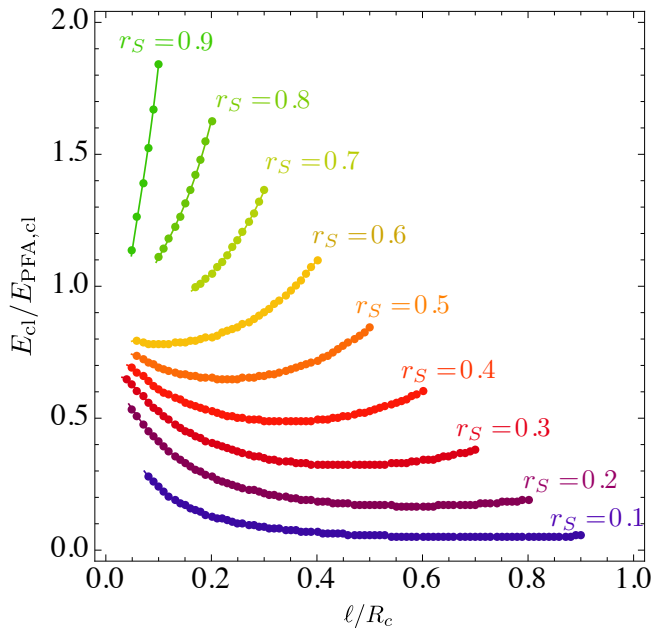

Figure 6. (Color online) Same as Fig. 5 for the classical high temperature limit.

for $\ell/R_c = 1 - R_s/R_c$). The sign of the corrections to the PFA depend on the ratio of the radii, $r_s = R_s/R_c$, in both the zero and the high temperature limit.

Corrections to the PFA can be computed in some cases by a derivative expansion [6]. This expansion can be used in the limit where the radii of curvature of the surfaces are much larger than their shortest distance, i.e., in the present geometry for R_s, $R_c \gg \ell$. By using the expansion for perfect conductors at $T = 0$, we obtain for the Casimir interaction at small $\ell \ll R_c$,

$$\mathcal{E}_0 = \mathcal{E}_{\rm PFA,0}\left[1 + \left(-1 - \frac{3}{2}r_s + r_s\sqrt{1-r_s} + \frac{2\beta + (2-3\beta)r_s + \beta r_s^2}{1-r_s}\right)\frac{1}{r_s}\frac{\ell}{R_c} + \ldots\right] \tag{62}$$

with $\beta = (2/3)(1 - 15/\pi^2)$[6]. The first correction to the PFA vanishes for $r_s = 0.4881$ where it changes sign which is consistent with the numerical results in Fig. 5. The numerical results approach the prediction of the derivative expansion at small surface-to-surface distance ℓ better for small r_s. Presumably, for larger r_s more multipoles need to be included in the numerical evaluation to obtain sufficient accuracy at short distances. In the classical limit, there exists no derivative expansion for perfect metals due to a non-analytic behavior of the kernel for small momenta [31].

V. CASIMIR INTERACTION OF TWO ATOMS INSIDE A CYLINDRICAL CAVITY

It is widely known that Casimir interactions are not pairwise additive: The energy of a system of a given number of objects is not the sum of the Casimir energies of all pairs. As a consequence, new phenomena can appear, as the non–monotonicity of the Casimir force for two cylinders [32], and for spheres or atoms in the presence of a perfect metal plate [33]. Similar effects can be expected for the interaction of objects inside cavities due to the confinement of field fluctuations. In particular, it is known that the Casimir force between two atoms which are confined between two dielectric parallel plates increases several orders of magnitude [34]. When the dielectric plates are replaced by perfect metal plates, the effect is even more pronounced: At zero temperature, the Casimir potential of the atoms decays no longer $\sim d^{-7}$ as in free space but $\sim d^{-5}$ [24]. In the high temperature limit, the Casimir potential was found to decay exponentially [25]. It is expected that the confinement effects increase with the degree of spatial confinement so that a cavity, e.g., a cylindrical shell should produce more pronounced consequences.

In this section we study the Casimir potential for two atoms inside a perfectly conducting cylindrical shell. We assume that the atoms have both electric and magnetic dipole polarizabilities. The Casimir energy of this 3-body problem is given by Eq. (1) with the block matrix

$$\mathcal{I} - \mathcal{N} = \begin{pmatrix} \mathcal{I} & -\mathcal{T}_{A_1}\mathcal{X}_{A_1A_2} & -\mathcal{T}_{A_1}\mathcal{X}_{A_1C} \\ -\mathcal{T}_{A_2}\mathcal{X}_{A_2A_1} & \mathcal{I} & -\mathcal{T}_{A_2}\mathcal{X}_{A_2C} \\ -\mathcal{T}_{C}\mathcal{X}_{CA_1} & -\mathcal{T}_{C}\mathcal{X}_{CA_2} & \mathcal{I} \end{pmatrix}, \tag{63}$$

where the matrix labels A_1, A_2 and C stand for atom 1, atom 2, and the cylindrical shell. For example, the matrix $\mathcal{X}_{CA_1}$ describes the translation between the cylindrical shell and atom 1. The determinant of this matrix can be rearranged using the

relations

$$\det\begin{bmatrix} A & B \\ C & D \end{bmatrix} = \det[A]\det\left[D - C\,A^{-1}\,B\right] = \det[D]\det\left[A - B\,D^{-1}\,C\right] . \quad (64)$$

The Casimir energy at zero temperature can then be written as

$$E_3 = \frac{\hbar c}{2\pi}\int_0^\infty d\kappa \log\left\{\det\left[\mathcal{I} - \mathcal{N}_{A_1C}\right]\det\left[\mathcal{I} - \mathcal{N}_{A_2C}\right]\det\left[\mathcal{I} - \mathcal{R}_{A_2A_1}\right]\right\} \quad (65)$$

where

$$\mathcal{N}_{A_1C} = \mathcal{T}_{A_1}\mathcal{X}_{A_1C}\mathcal{T}_C\mathcal{X}_{CA_1} , \quad (66)$$

$$\mathcal{N}_{A_2C} = \mathcal{T}_{A_2}\mathcal{X}_{A_2C}\mathcal{T}_C\mathcal{X}_{CA_2} , \quad (67)$$

$$\mathcal{R}_{A_2A_1} = \mathcal{T}_{A_1}\left(\mathcal{X}_{A_1A_2} + \mathcal{X}_{A_1C}\mathcal{T}_C\mathcal{X}_{CA_2}\right)\left(\mathcal{I} - \mathcal{N}_{A_2C}\right)^{-1}\mathcal{T}_{A_2}\left(\mathcal{X}_{A_2A_1} + \mathcal{X}_{A_2C}\mathcal{T}_C\mathcal{X}_{CA_1}\right)\left(\mathcal{I} - \mathcal{N}_{A_1C}\right)^{-1} . \quad (68)$$

The first two matrices describe the interaction of each atom with the cavity, and the third matrix describes the interaction between the two atoms, taking into account the presence of the cavity. In the absence of the cavity, the latter matrix reduces to $\mathcal{R}_{A_2A_1} = \mathcal{T}_{A_1}\mathcal{X}_{A_1A_2}\mathcal{T}_{A_2}\mathcal{X}_{A_2A_1}$ which describes two atoms in free space.

It is convenient to express the matrix $\mathcal{R}_{A_2A_1} \equiv \mathcal{R}$ in spherical multipole basis which reads

$$\mathcal{R}_{lm,l''m''} = \mathcal{T}_{A_1\,lm,lm}\tilde{\mathcal{U}}_{A_1A_2\,lm,l'm'}(d,\mathbf{X}_{12})\mathcal{T}_{A_2\,l'm',l'm'}\tilde{\mathcal{U}}_{A_2A_1\,l'm',l''m''}(d,\mathbf{X}_{21}), \quad (69)$$

where here and in the following repeated indices are summed over. Here d is the distance between the atoms and the axis of the cylindrical cavity, and $\tilde{\mathcal{U}}_{A_\alpha A_\beta\,lm,l'm'}(d,\mathbf{X}_{\alpha\beta})$ are the modified translation matrices for the translation by the vector $\mathbf{X}_{\alpha\beta} \equiv \pm h\hat{\mathbf{z}}$ along the cylinder axis from atom α to atom β. They are defined by

$$\tilde{\mathcal{U}}_{A_\alpha A_\beta\,lm,l'm'}(d,\mathbf{X}_{\alpha\beta}) = \left(\mathcal{U}_{A_\alpha A_\beta\,lm,l''m''}(\mathbf{X}_{\alpha\beta}) + D_{lm,nk_z}\mathcal{V}_{A_\alpha C\,nk_z,n'k_z}\mathcal{T}_{C\,n'k_z,n'k_z}\mathcal{V}^\dagger_{CA_\beta\,n'k_z,n''k_z}D^\dagger_{n''k_z,l''m''}\frac{C^c}{C^s}\right) \times \left(\mathcal{I} - \mathcal{N}_{A_\beta C}\right)^{-1}_{l''m'',l'm'} , \quad (70)$$

where $\mathcal{N}_{A_\beta C} = \mathcal{T}_{A_\beta}\mathcal{X}_{A_\beta C}\mathcal{T}_C\mathcal{X}_{CA_\beta}$ describes the Casimir interaction of an atom with the cylindrical cavity, and the constants C^c and C^s are defined below Eq. (7). The translation matrices $\mathcal{U}$ are defined in App. A. Note that the polarization indices and the integral over k_z are not shown explicitly.

In the following, we are interested in the interaction between the two atoms (and not the change of energy when the atoms are moved away from the cylinder axis). This interaction is given by the last determinant of Eq. (65) and hence by the matrix $\mathcal{R}$. Under the two assumptions formulated in the beginning of Sec. III, we need to retain only the contribution linear in $\mathcal{R}$ so that the Casimir energy is given by

$$E_T = k_BT{\sum_{n=0}^{\infty}}' \mathrm{Tr}\left[\tilde{\mathcal{R}}(\kappa_n)\right] , \quad (71)$$

where $\tilde{\mathcal{R}}$ is defined by the (symbolic) expression

$$\tilde{\mathcal{R}} = \mathcal{T}_{A_2}\left(\mathcal{U}_{A_2A_1} + D\mathcal{V}_{A_2C}\mathcal{T}_C\mathcal{V}^\dagger_{CA_1}D^\dagger\right) \times \mathcal{T}_{A_1}\left(\mathcal{U}_{A_1A_2} + D\mathcal{V}_{A_1C}\mathcal{T}_C\mathcal{V}^\dagger_{CA_2}D^\dagger\right) , \quad (72)$$

that is the simplification of $\mathcal{R}$ correct to linear order in the polarizabilities of the atoms. The matrix $\tilde{\mathcal{R}}$ has four contributions that can be understood as distinct scattering processes. The two terms containing $\mathcal{U}$ describe direct scattering between the two atoms not involving the cylindrical cavity. The other two terms containing $\mathcal{T}_C$ correspond to indirect scattering between the atoms with a reflection at the cylindrical cavity.

In the following, we consider the zero and high temperature classical limit of the interaction between the atoms that are located on the cylinder axis and have separation h. In these two limits, the Casimir interaction energies can be written as

$$E_0 = -\frac{\hbar c}{4\pi R_c^7}\left[e_0^{EE}(\eta)\alpha_1^E\alpha_2^E + e_0^{MM}(\eta)\alpha_1^M\alpha_2^M + e_0^{EM}(\eta)\left(\alpha_1^E\alpha_2^M + \alpha_1^M\alpha_2^E\right)\right] , \quad (73)$$

$$E_{cl} = -\frac{k_BT}{R_c^6}\left[e_{cl}^{EE}(\eta)\alpha_1^E\alpha_2^E + e_{cl}^{MM}(\eta)\alpha_1^M\alpha_2^M\right] , \quad (74)$$

respectively, with $\eta = h/R_c$. Here α_j^P are the dipolar electric ($P = E$) and magnetic ($P = M$) polarizabilities of the atoms. Note that there are no terms proportional to $\alpha_i^E\alpha_j^M$ in the high temperature limit. Below, we shall give analytical and numerical results for the amplitude functions e_0 and e_{cl} in various limiting cases.

A. Retarded limit

We first consider the situation where the distance between the atoms is much bigger than the retardation length, $h \gg d_{10}$. This corresponds to the so-called Casimir–Polder or retarded limit.

1. *Zero temperature*

Indeed, when thermal effects are unimportant and the distance $h \ll R_c$, the atoms interact as in free space, and we obtain the usual Casimir–Polder potential for two atoms at zero temperature, corresponding to

$$e_0^{EE}(\eta) = e_0^{MM}(\eta) = \frac{23}{\eta^7}, \tag{75}$$

$$e_0^{EM}(\eta) = -\frac{7}{\eta^7}\,. \tag{76}$$

In the opposite limit where $h \gg R_c \gg d_{10}$ the atoms experience the confinement by the cylindrical shell, leading to an exponential decay of their interaction. For $\eta \gg 1$, we obtain the limiting amplitude functions

$$e_0^{MM} = \frac{\sqrt{\pi^9 {j'_{1,1}}^{21}} {Y'_1}^4(j'_{1,1})}{8\left({j'_{1,1}}^2 - 1\right)^2} \frac{e^{-2j'_{1,1}\eta}}{\eta^{1/2}} = 286.20 \frac{e^{-2j'_{1,1}\eta}}{\eta^{1/2}}\,, \tag{77}$$

$$e_0^{EE} = \frac{3\sqrt{\pi^9 {j'_{1,1}}^{17}} {Y'_1}^4(j'_{1,1})}{32\left({j'_{1,1}}^2 - 1\right)^2} \frac{e^{-2j'_{1,1}\eta}}{\eta^{5/2}} = 63.32 \frac{e^{-2j'_{1,1}\eta}}{\eta^{5/2}}\,, \tag{78}$$

$$e_0^{EM} = -\frac{8\sqrt{2}\pi^2 {j'_{1,1}}^4 {Y'_1}^2(j'_{1,1})}{{j'_{1,1}}^2 - 1} \frac{e^{-j'_{1,1}\eta}}{\eta^5} = -189.59 \frac{e^{-j'_{1,1}\eta}}{\eta^5}\,, \tag{79}$$

where $j'_{1,1} = 1.84118$ is the lowest zero of the derivative of the Bessel functions of first kind, $J'_1(x)$, and $Y'_1(x)$ is the derivative of a Bessel function of second type. The electromagnetic fluctuations inside the confining cylinder are effectively massive with a mass $\sim R_c$ that produces the exponential decay of the interaction for $h \gg R_c$. We have evaluated the amplitude functions $e_0(\eta)$ for intermediate values of η numerically. The results are shown in Fig. 7 for the three possible combinations of the polarizations. Shown in the plots are also the limiting analytical results of Eqs. (75), (76), (77), (78), (79). One can clearly observe the crossover between the two limiting expressions for $h \ll R_c$ and $h \gg R_c$.

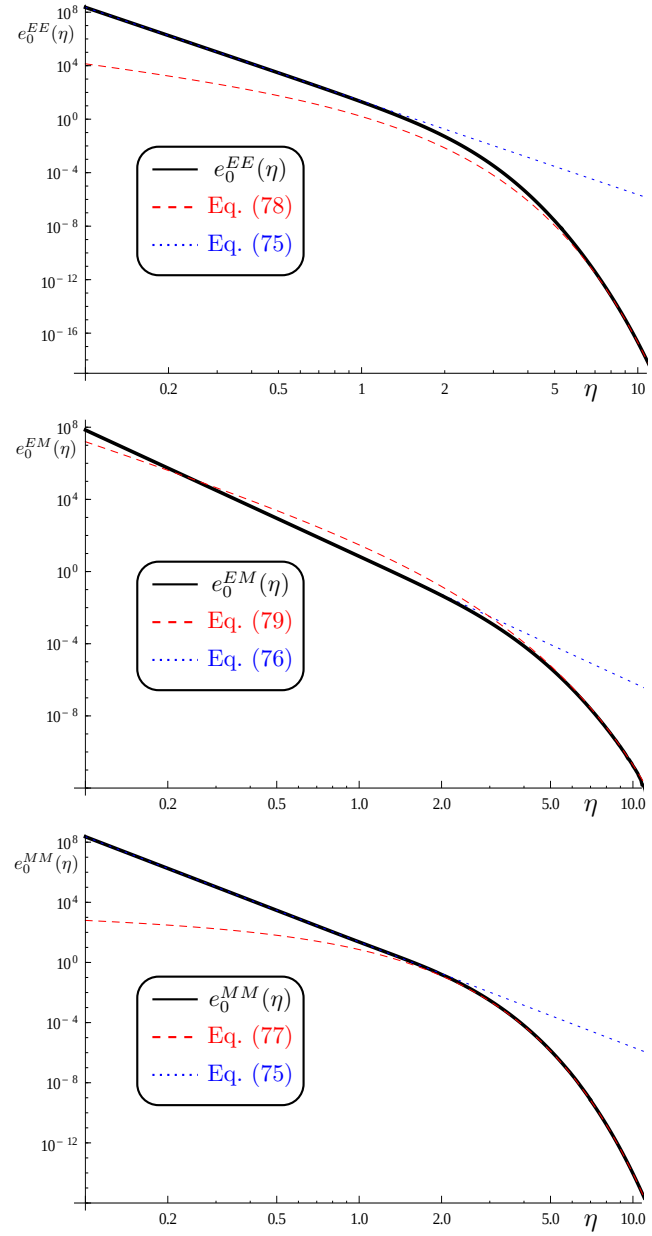

Figure 7. (Color online) Log–log plot of the numerical results for the functions $e_0(\eta)$ as a function of $\eta = h/R_c$ for the three combinations of polarizations (solid curves). The dashed curves represent the large distance limits ($\eta \gg 1$) given by Eqs. (77), (78) and (79), and the dotted curves correspond to the short distance limits ($\eta \ll 1$) given by Eqs. (75) and (76)).

2. *High temperature limit*

Next, we consider the retarded regime in the high temperature classical limit. In this case, the electric and magnetic polarizations do not couple, as indicated already in Eq. (74). For short distances, $h \ll R_c$, we recover the classical limit of the Casimir–Polder potential, corresponding to

$$e_{cl}^{EE}(\eta) = e_{cl}^{MM}(\eta) = \frac{3}{\eta^6}\,. \tag{80}$$

In the large distance limit, $h \gg R_c \gg d_{10}$, the potential decays again exponentially due to the confinement,

$$e_{cl}^{EE} = \frac{\pi^4 j_{0,1}^6 Y_0^4(j_{0,1})}{8} e^{-2j_{0,1}\eta} = 159.23 e^{-2j_{0,1}\eta}\,, \quad (81)$$

$$e_{cl}^{MM} = \frac{\pi^4 {j'_{1,1}}^{10} {Y'_1}^4(j'_{1,1})}{16\left({j'_{1,1}}^2 - 1\right)^2} e^{-2j'_{1,1}\eta} = 59.50 e^{-2j'_{1,1}\eta}\,, \quad (82)$$

where $j_{0,1} = 2.40483$ is the lowest zero of the Bessel function of the first kind $J_0(x)$.

To obtain information about intermediate distances, we have evaluated the amplitude functions $e_{cl}(\eta)$ also numerically. The results are shown in Fig. 8, together with the analytical results for large and small distances. The plots show that the limiting analytical results merge at η of order unity and yield an accurate description of the interaction between the atoms for the entire range of separations.

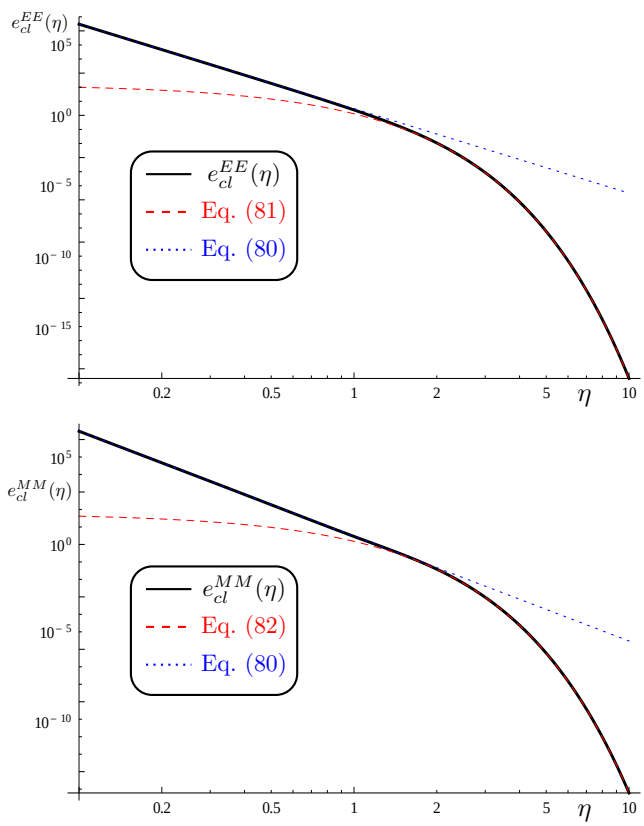

Figure 8. (Color online) Log–log plot of the numerical results for the functions $e_{cl}(\eta)$ as a function of $\eta = h/R_c$ for the two combinations of polarizations (solid curves). The dashed curves represent the large distance limits ($\eta \gg 1$) given by Eqs. (81) and (82), and the dotted curves correspond to the short distance limits ($\eta \ll 1$) given by Eq. (80)

.

B. Non–retarded limit

Finally, we consider the non–retarded limit where h, $R_c \ll d_{10}$ but $\eta = h/R_c$ is arbitrary. In this limit, the interaction between the atoms is usually referred to as London force. Formally, this case corresponds to an infinite velocity of light, $c \to \infty$. Here we consider arbitrary temperatures T. Following the steps carried out in Sec. III B, we can carry out the Matsubara sum and obtain the London potential

$$E_T^L(\eta) = f\left(\frac{\hbar\omega_{10}}{k_B T}\right) E_{cl}(\eta), \quad (83)$$

where the coefficient function $f(t)$ is given by

$$f(t) = \frac{t}{4}\frac{t + \sinh(t)}{\cosh(t) - 1} \quad (84)$$

and $E_{cl}(\eta)$ is the high temperature limit of the Casimir energy given by Eqs. (74), (80). Similar to the interaction between a single atom and a cylinder, the non-retarded interaction at finite temperature is related to the classical limit of the retarded interaction. Note that in the zero and high temperature limit of the London potential we have

$$E_0^L(\eta) = \frac{\hbar\omega_{10}}{4k_B T} E_{cl}(\eta)\,, \quad (85)$$

$$E_{cl}^L(\eta) = E_{cl}(\eta)\,. \quad (86)$$

VI. DISCUSSION

We have studied how curvature and in particular confinement can effectively modify Casimir interactions between an atom and a curved surface and between atoms confined in perfectly conducting cylindrical cavities. For the interaction between a single atom and a cylindrical shell we have developed both large and short distance expansions that apply in the zero and high temperature limits, and for an interior and exterior atom. The expansions agree nicely with a full numerical evaluation at arbitrary atom-surfaces distances. Our results are relevant to understanding the scattering of atoms at curved surfaces, e.g., nanotubes. We have considered both the retarded and non-retarded limits. For the latter, we have shown that it is simply related to the classical (high temperature) limit of the Casimir-Polder potential.

A problem with a higher degree of complexity is the interaction of a macroscopic spherical particle with a confining cylindrical shell. We have considered the limit of perfect conductivity for both the particle and the shell. By computing the interaction numerically from a large number of multipole moments, we were able to compare to the proximity force approximation (PFA) and its correction as predicted by a gradient expansion. We found nice agreement, confirming that the gradient expansion makes reliable predictions also for interior problems.

We have shown that the Casimir-Polder interaction of two atoms is modified when the atoms are confined by perfectly

conducting cylindrical shell, and their distance is comparable or larger than the radius of the shell. This is due to the fact that Casimir interactions are not pairwise additive. We have considered the limits of zero and high temperature, both in the retarded and non-retarded cases. In all situations, the interaction is substantially reduced compared to free space and decays exponentially over the scale of the radius of the shell. Although we assumed a perfectly conducting cylindrical shell, we expect that our conclusion remain qualitatively unchanged for general dielectric materials.

The impact of boundary effects on the force between a pair of atoms at zero temperature have been studied originally by Mahanty and Ninham [24], showing a reduced force in the non-retarded limit and an increased force in the retarded limit. At any finite temperature, an exponentially reduced force was found [25]. More recently, there have been studies of the Casimir-Polder interaction for an atom inside a cylindrical cavity [30, 35], and a compact object inside a spherical cavity [9]. Recent studies of the modification of the force between two atoms inside quasi one-dimensional structures have displayed an exponential reduction of the interaction for a rectangular waveguide [26] and a huge amplification of the interaction for two concentric metallic cylinders[27]. The observed exponential decay could be explained in terms of evanescent modes and related to existing prediction in the literature.

It seems that confinement leads to reduction or amplification of inter-molecular fluctuation forces and has important consequences for the (non-)additivity of these forces, and hence the electromagnetic response of confined gases. Clearly, all modes in our cylindrical shell, and also in the rectangular waveguide of Ref. [26] are massive, explaining an exponential reduction of the interaction. Since this propagating mode contributes for two particles with electric polarizability only in the retarded limit, However, the interaction between two particle between two parallel conducting plates is not exponentially suppressed but enhanced in the retarded limit as in this regime there exists a massless mode for TM polarization [28] similar to the situation of the transmission line. It would be interesting to establish corresponding results for non-equilibrium effects in confined geometries.

ACKNOWLEDGMENTS

The research leading to these results has received funding from the People Programme (Marie Curie Actions) of the European Union's Seventh Framework Programme (FP7/2007-2013) under REA grant agreement n° 302005. P. R.-L. acknowledge helpful discussions with A. A. Saharian. P. R.-L.'s research has also been supported by Projects MOSAICO, UCM (Grant No. PR34/07-15859), MODELICO (Comunidad de Madrid), ENFASIS (Grant No.FIS2011-22644, Spanish Government) in the Departamento de Física Aplicada I and GISC of the Facultad de Ciencias Físicas of the Universidad Complutense of Madrid, by "Ministerio de Economía y Competitividad" (Spain) Grant No. FIS2012-38866-C05-01 in the Departamento de Matemáticas and GISC of the Universidad Carlos III de Madrid, by the Engineering and Physical Sciences Research Council under EP/H049797/1 in the Department of Physics of the Loughborough University. This work was supported by the National Science Foundation through Grant No. DMR-1310687 (RZ).

Appendix A: Matrix elements

Here we provide explicit expressions for the elements of the various matrices of the scattering approach for imaginary wave numbers $k = i\kappa$.

1. Conversion matrices

The elements of the conversion matrices from spherical vector multipoles to cylindrical vector multipoles are [22]

$$D_{lmM,nk_zM} = C_{lm}\frac{\sqrt{\kappa^2+k_z^2}}{\kappa}P_l^{m\prime}\left(-i\frac{k_z}{\kappa}\right)\delta_{nm}, \quad \text{(A1)}$$

$$D_{lmE,nk_zM} = C_{lm}\frac{\kappa}{\sqrt{\kappa^2+k_z^2}}imP_l^{m}\left(-i\frac{k_z}{\kappa}\right)\delta_{nm}, \quad \text{(A2)}$$

$$D_{lmM,nk_zE} = -D_{lmE,nk_zM}, \quad \text{(A3)}$$

$$D_{lmE,nk_zE} = D_{lmM,nk_zM}, \quad \text{(A4)}$$

where

$$C_{lm} = (-1)^{l-m}\frac{4\pi}{\sqrt{l(l+1)}}\sqrt{\frac{2l+1}{4\pi}\frac{(l-m)!}{(l+m)!}}. \quad \text{(A5)}$$

2. T–matrix of a perfect metal sphere

For a perfect sphere of radius R_s, the T–matrix elements are well known. In the spherical wave basis they are given in terms of the Bessel functions I_l and K_l by [12],

$$\mathcal{T}_{S\ lmM,l'm'M} = -\delta_{ll'}\delta_{mm'}\frac{\pi}{2}\frac{I_{l+\frac{1}{2}}(\kappa R_s)}{K_{l+\frac{1}{2}}(\kappa R_s)}, \quad \text{(A6)}$$

$$\mathcal{T}_{S\ lmN,l'm'N} = -\delta_{ll'}\delta_{mm'}\frac{\pi}{2}\frac{lI_{l+\frac{1}{2}}(\kappa R_s)-\kappa R_s I_{l-\frac{1}{2}}(\kappa R_s)}{lK_{l+\frac{1}{2}}(\kappa R_s)+\kappa R_s K_{l-\frac{1}{2}}(\kappa R_s)}, \quad \text{(A7)}$$

and the elements coupling unlike polarizations vanish.

3. T–matrix of an atom

The T–matrix of a two-state atom can be expressed in terms of its dipolar polarizability as a diagonal matrix, whose non–vanishing elements are

$$\mathcal{T}_{S\ 1,m,M;1,m',M} = -\delta_{m,m'}\frac{2\kappa^3}{3}\alpha_1^{MM}, \quad \text{(A8)}$$

$$\mathcal{T}_{S\ 1,m,N;1,m',N} = -\delta_{m,m'}\frac{2\kappa^3}{3}\alpha_1^{EE}, \quad \text{(A9)}$$

where the electric and magnetic polarizabilities at imaginary frequency κ are given by

$$\alpha_1^{EE} = \frac{\alpha_E}{1 + d_{10}^2 \kappa^2}, \tag{A10}$$

$$\alpha_1^{MM} = \frac{\alpha_M}{1 + d_{10}^2 \kappa^2}, \tag{A11}$$

and $d_{10} = c/\omega_{10}$ with the transition frequency ω_{10}.

4. T–matrix of a perfect metal cylinder

We need the T-matrix of a perfect metal cylinder for both exterior and interior scattering. For the case of exterior scattering, the non-vanishing elements are given by

$$\mathcal{T}_{C\ nk_zN,n'k_z'N} = -\delta(k_z - k_z')\delta_{nn'} \frac{I_n(R_c p)}{K_n(R_c p)}\,, \tag{A12}$$

$$\mathcal{T}_{C\ nk_zM,n'k_z'M} = -\delta(k_z - k_z')\delta_{nn'} \frac{I_n'(R_c p)}{K_n'(R_c p)}\,, \tag{A13}$$

where $p = \sqrt{k_z^2 + \kappa^2}$ and R_c is the radius of the cylinder. For the case of interior scattering the elements are obtained by inversion of the elements for the exterior case,

$$\mathcal{T}_{C\ nk_zN,n'k_z'N} = -\delta(k_z - k_z')\delta_{nn'} \frac{K_n(R_c p)}{I_n(R_c p)}\,, \tag{A14}$$

$$\mathcal{T}_{C\ nk_zM,n'k_z'M} = -\delta(k_z - k_z')\delta_{nn'} \frac{K_n'(R_c p)}{I_n'(R_c p)}\,. \tag{A15}$$

5. Cylindrical translation matrices

The translation matrices that relate regular cylindrical waves to regular cylindrical waves with respect to a displaced origin are diagonal in the polarization with the non-vanishing elements given by [12]

$$\mathcal{V}_{SC\ nk_z,n'k_z'} = (-1)^{n+n'} I_{n-n'}(d\sqrt{k_z^2 + \kappa^2}) e^{-i(n-n')\theta_{SC}} \times e^{-ik_z X_{SC,z}} \delta(k_z - k_z'), \tag{A16}$$

$$\mathcal{V}^{\dagger}_{CS,\ nk_z,n'k_z'} = (-1)^{n+n'} I_{n-n'}(d\sqrt{k_z^2 + \kappa^2}) e^{-i(n-n')\theta_{CS}} \times e^{ik_z X_{CS,z}} \delta(k_z - k_z'), \tag{A17}$$

where $\theta_{CS} = \theta_{SC} \pmod{2\pi}$. The elements of the matrix relating regular to outgoing waves (relevant to exterior scattering between two objects A_1 and A_2) are given by

$$\mathcal{U}_{A_1A_2\,nk_z,n'k_z'} = (-1)^{n'} K_{n-n'}(d\sqrt{k_z^2 + \kappa^2}) e^{-i(n-n')\theta_{A_1A_2}} \times e^{-ik_z X_{A_1A_2,z}} \delta(k_z - k_z'). \tag{A18}$$

6. Spherical translation matrices

It turns out that it is useful for the computations presented in the main text to express the translation matrices for spherical waves in terms of those for cylindrical waves, using the conversion matrices $D_{l\,m\,Q,n\,k_z\,P}$. The elements of the spherical translation matrix can then be written as

$$\mathcal{U}_{A_1A_2\,l\,m\,Q,\tilde{l}\tilde{m}\tilde{Q}} = \sum_{n,n',P} \int_{-\infty}^{\infty} \frac{dk_z}{2\pi} \int_{-\infty}^{\infty} \frac{dk_z'}{2\pi} D_{l\,m\,Q,n\,k_z\,P} \times \mathcal{U}_{A_1A_2\,n\,k_z,n'\,k_z'} D^{\dagger}_{n'\,k_z'\,P,\tilde{l}\tilde{m}\tilde{Q}} \frac{C_P^c}{C_{\tilde{Q}}^s}. \tag{A19}$$

Taking into account that the cylindrical translation matrix is diagonal in k_z, we can carry out the integral over k_z'. Finally, the translation matrices in spherical waves can be found in [12].

[1] F. London, Trans. Faraday Soc. **33**, 8 (1937).
[2] H. B. G. Casimir and D. Polder, Phys. Rev. **73**, 360 (1948).
[3] F. M. Serry, D. Walliser, and G. J. Maclay, Journal of Applied Physics **84**, 2501 (1998).
[4] G.L. Klimchitskaya, U. Mohideen, and V.M. Mostepanenko, Rev. Mod. Phys. **81**, 1827 (2009).
[5] D. Dalvit, P. Milonni, D. Roberts, and F. Rosa, eds., Lecture Notes in Physics, Casimir Physics, vol. 834 (Springer, 2011).
[6] G. Bimonte and T. Emig and R. L. Jaffe and M. Kardar, EPL **97** 50001 (2012).
[7] M. F. Maghrebi, S. J. Rahi, T. Emig, N. Graham, R. L. Jaffe, and M. Kardar, PNAS **108**, 6867 (2011).
[8] T. Emig, N. Graham, R. L. Jaffe, and M. Kardar, Phys. Rev. A **79**, 054901 (2009).
[9] S. Zaheer, S. J. Rahi, T. Emig and R. L. Jaffe. Phys. Rev. A **82**, 052507 (2010).
[10] D. A. R. Dalvit, F. C. Lombardo, F. D. Mazzitelli, and R. Onofrio, Phys. Rev. A **74**, 020101(R) (2006).
[11] T. Emig, N. Graham, R.L. Jaffe and M. Kardar. Phys. Rev. Lett. **99**, 170403 (2007).
[12] S. J. Rahi, T. Emig, N. Graham, R. L. Jaffe, and M. Kardar. Phys. Rev. D **80**, 085021 (2009).
[13] A. Lambrecht P. A. Maia Neto and S. Reynaud. *New Journal of Physics* **8**, 243 (2006).
[14] O. Kenneth and I. Klich. Phys. Rev. B **78**, 014103 (2008).
[15] A. Bulgac, P. Magierski, and A. Wirzba. Phys. Rev. D **73**, 025007 (2006).
[16] E. Noruzifar, T. Emig, and R. Zandi, Phys. Rev. A **84**, 042501 (2011).
[17] E. Noruzifar, T. Emig, U. Mohideen, and R. Zandi, Phys. Rev. B **86**, 115449 (2012).

[18] T. Emig, R. L. Jaffe, M. Kardar, and A. Scardicchio, Phys. Rev. Lett. **96**, 080403 (2006).

[19] S. J. Rahi, T. Emig, R. L. Jaffe, and M. Kardar, Phys. Rev. A **78**, 012104 (2008).

[20] R. Zandi, T. Emig, and U. Mohideen, Phys. Rev. B **81**, 195423 (2010).

[21] P. Rodriguez-Lopez and T. Emig, Phys. Rev. A **85**, 032510 (2012).

[22] E. Noruzifar, P. Rodriguez-Lopez, T. Emig and R. Zandi. Phys. Rev. A **87**, 042504 (2013).

[23] L. P. Teo. Phys. Rev. D **87**, 045021 (2013).

[24] J. Mahanty and B. W. Ninham. J. Phys. A: Math., Nucl. Gen. **6**, 1140 (1973).

[25] M. Boström, J. J. Longdell and B. W. Ninham. Phys. Rev. A **64**, 062702 (2001).

[26] E. Shahmoon and G. Kurizki. Phys. Rev. A **87**, 062105 (2013).

[27] E. Shahmoon, I. Mazets, and G. Kurizki, PNAS **111**, 10485 (2014).

[28] P. W. Milonni, *The quantum vacuum : an introduction to quantum electrodynamics* (Academic Press, 1994)

[29] X. Pan, Z. Fan, W. Chen, Y. Ding, H. Luo and X. Bao, Nature Materials **6**, 507 - 511 (2007).

[30] V.B. Bezerra, E.R. Bezerra de Mello, G.L. Klimchitskaya, V.M. Mostepanenko, and A.A. Saharian. Eur. Phys. J. C **71**:1614 (2011).

[31] C. D. Fosco, F. C. Lombardo, and F. D. Mazzitelli, Phys. Rev. D **86**, 045021 (2012).

[32] S. J. Rahi, A. W. Rodriguez, T. Emig, R. L. Jaffe, S. G. Johnson and M. Kardar. Phys. Rev. A **77**, 030101 (2008).

[33] P. Rodriguez-Lopez, S. J. Rahi and T. Emig. Phys. Rev. A **80**, 022519 (2009).

[34] M. Marcovitch and H. Diamant. Phys. Rev. Lett. **95**, 223203 (2005).

[35] S. Å. Ellingsen, S. Y. Buhmann and S. Scheel. Phys. Rev. A **82**, 032516 (2010).